SLAS Technology 27 (2022) 54–62

Contents lists available at ScienceDirect

SLAS Technology

journal homepage: www.elsevier.com/locate/slast

Quantitative determination of uric acid using paper-based biosensor modified with graphene oxide and 5-amino-1,3,4-thiadiazole-2-thiol

Yaw-Jen Chang[a,*], Ming-Che Lee[a], You-Chiuan Chien[a,b]

[a] Department of Mechanical Engineering, Chung Yuan Christian University, Chung Li District, Taoyuan City, 32023, Taiwan
[b] Changhua Christian Hospital, Changhua City, Changhua County 500, Taiwan

ARTICLE INFO

Keywords:
Uric acid
5-Amino-1,3,4-thiadiazole-2-thiol (ATT)
Graphene oxide
Cyclic voltammetry

ABSTRACT

Uric acid is the primary end product of human purine metabolism and has been regarded as a key parameter in urine and blood for monitoring physiological conditions. This paper presents a paper-based biosensor for a quantitative determination of uric acid using electrochemical detection. The working electrode of the biosensor is modified with graphene oxide (GO) and 5-amino-1,3,4-thiadiazole-2-thiol (ATT) by electropolymerizing ATT on the surface of graphene oxide. In this study, cyclic voltammetry (CV) measurements required only 200 μL of analyte solution. The experimental results showed that the oxidation peak current increased as the concentration of uric acid become higher and exhibited a linear relationship in the concentration range of 0.1–10 mM, indicating that this proposed biosensor has high sensitivity. In addition, this biosensor has good selectivity to detect uric acid because ATT has a specific binding with it. In human blood and body fluids, nitrites may be the only factor that can interfere with the detection of uric acid using this proposed biosensor. Nevertheless, uric acid can be discriminated from nitrite in the CV measurement due to different oxidation potentials. Thus, this proposed paper-based biosensor is a promising tool for detecting uric acid in biological samples.

Introduction

Uric acid (UA) is the primary end product of human purine metabolism. While approximately 70% of daily uric acid is disposed of through the kidneys as a component of urine, the rest is recirculated into the blood system. In general, uric acid has homeostatic solubility in human serum. When the homeostasis of uric acid is interfered with, some physiological disorders may occur. Hence, uric acid has been regarded as a key parameter in urine and blood for monitoring physiological conditions and an important diagnostic biomarker for several systemic diseases.

Since purine is disintegrated into uric acid, the UA concentration is related to purine metabolism and normally remains in a stable range for healthy persons. The normal concentration of uric acid present in the blood is in the range of 3–7 mg/dL, whereas that excreted in the urine is about 16–100 mg/dL per 24 h. [1–3] A high purine intake from diet produces an excessive amount of uric acid in the human body. When the excessive uric acid gets concentrated and crystallized, the crystallites cause numerous illnesses. Gout is such an ailment caused by the deposition of crystallites of uric acid in human joints. Besides, excessive uric acid levels are key pathogenesis of several diseases, including hyperuricemia (i.e., high UA concentration), heavy hepatitis, Lesch–Nyan syndrome, cardiovascular diseases, gouty arthritis, UA urolithiasis, even chronic renal diseases. A high level of uric acid in the blood is a serious problem for health. The prevalence rate of hyperuricemia is rising on a global scale, imposing a growing disease burden in healthcare systems. [4] Conversely, an abnormally low uric acid level can also cause other diseases, such as multiple sclerosis. In other words, variations in uric acid concentration might result in physiological disorders. Quantitative determination of uric acid is of great importance for clinical needs in disease diagnosis and medicine control.

Various analytical approaches have been proposed to detect uric acid, including spectrophotometry, [5] electrochemiluminescence (also called electrogenerated chemiluminescence, ECL), [6–8] surface-enhanced Raman spectroscopy (SERS), [3,9] electrochemical analysis, [10–12] etc. Recently, electrochemical techniques have become remarkable methods in detecting uric acid because these techniques exhibit simplicity and great sensitivity based on the interaction of electrical energy and matter. Nevertheless, an electrode's surface modification is key to improving selectivity in detecting electrochemically active compounds. [13,14] In the literature, the electrodes modified with carbon nanotubes, nanoparticles, and electroactive polymers have been studied for detecting uric acid or simultaneous determination of ascorbic acid, dopamine, and uric acid. [15–17]

However, most of these methods for surface modifications rely on expensive instruments or require sophisticated processes. Furthermore,

* Corresponding author.
E-mail address: justin@cycu.edu.tw (Y.-J. Chang).

https://doi.org/10.1016/j.slast.2021.10.010

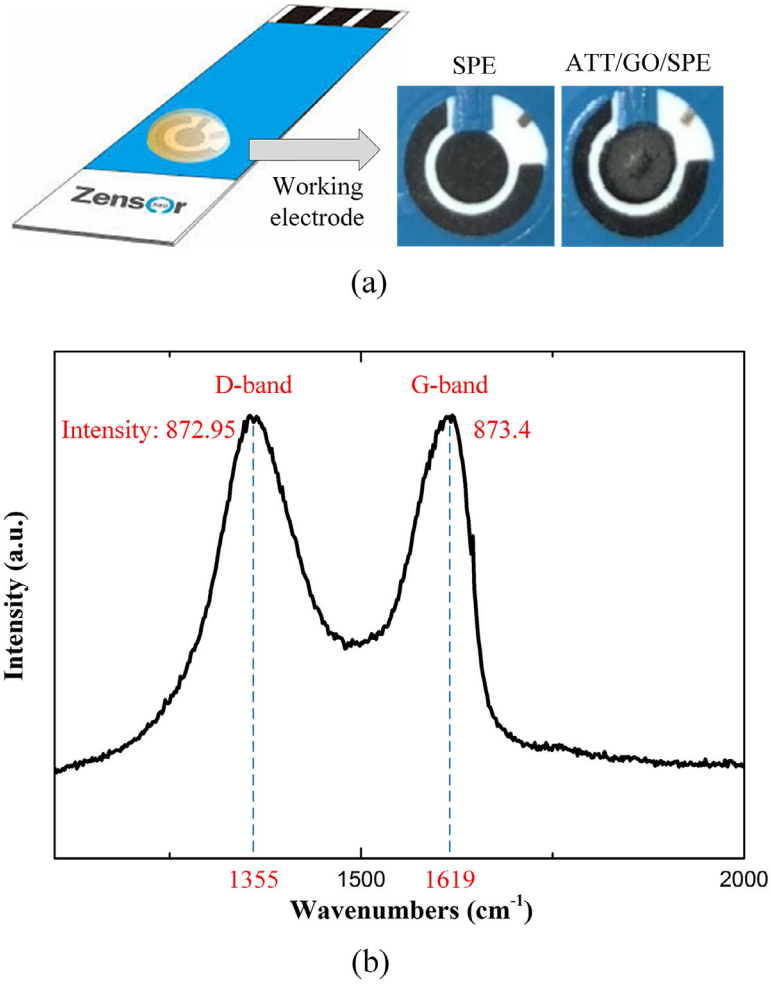

Fig. 1. (a) The paper-based biosensor modified with graphene oxide and 5-amino-1,3,4-thiadiazole-2-thiol (ATT). (b) Raman spectrum of graphene oxide.

uric acid usually coexists with ascorbic acid and dopamine in biological fluids, such as blood and urine. They all are electroactive compounds, playing an important role in human metabolism. This phenomenon becomes a major obstacle in detecting uric acid from other electroactive constituents. That is, these electroactive compounds may interfere in the measurement of uric acid. For instance, the oxidation potential of ascorbic acid is close to that of uric acid. Therefore, the development of a biosensor with excellent sensitivity and selectivity to quantitatively determine the uric acid level is highly desirable.

In this work, a paper-based biosensor with electrochemical detection for a quantitative determination of uric acid has been developed. The working electrode of the paper-based biosensor is modified with graphene oxide (GO) and 5-amino-1,3,4-thiadiazole-2-thiol (ATT). GO is an oxidized form of graphene laced with oxygen-containing groups, such as epoxide, carboxyl, and hydroxyl functional groups on carbon surface. It has many fascinating properties, such as a large surface-to-volume ratio, superior chemical stability, and excellent biocompatibility. Thus, GO was generally applied as a coating on substrates in sensor applications. [18–25] Furthermore, ATT is a chemical compound used to detect orange II, anthracene-9-carbonxylic acid (9-ACA), nitrite, etc., by electropolymerization on the electrode. [26–28] For certain substances, ATT can provide specific bonding with them. Additionally, paper-based sensors have attracted the attention of researchers as they are portable, disposable, and inexpensive. [29–31] Since the oxygen-containing groups in GO are reactive, the mechanism of this proposed paper-based biosensor is to utilize GO to immobilize ATT for the detection of uric acid. This biosensor requires a small amount of sample. Moreover, the adsorption of ATT and the characteristics of this sensor in detecting uric acid have been systematically studied.

Materials and methods

Materials

The paper-based chip was purchased from Zensor R&D Corp. (Taiwan). It has three screen-printed carbon electrodes (SPEs) for electrochemical measurement. Uric acid (2,6,8-Trihydroxypurine, $C_5H_4N_4O_3$, 99% extra pure powder) purchased from SIGMA-Aldrich was used as the analyte. In addition, 5-amino-1,3,4-thiadiazole-2-thiol (=$C_2H_3N_3S_2$, ATT) purchased from Tokyo Chemical Industry (Japan) was used to capture uric acid for determining its level. Phosphate buffered saline (PBS) was used to prepare the ATT solution.

On the electrode of the paper-based chip, a layer of graphene oxide was coated to immobilize ATT. The materials necessary for synthesizing the graphene oxide include graphite (purchased from SIGMA-Aldrich), H_2SO_4, $NaNO_3$, $KMnO_4$, H_2O_2, and dialysis membrane. The reagents for the anti-interference study include ascorbic acid, nitrite, glucose, dopamine, and red blood cell. Ascorbic acid ($C_6H_8O_6$) was purchased from Ferak Berlin; nitrite was obtained from Pure Chemicals Co.; glucose and dopamine were purchased from SIGMA-Aldrich. Antibody screening cell, the substitute for RBC in human blood, was purchased from Formosa Biomedical Technology Corp. (Taiwan).

Electropolymerization of ATT

Prior to the immobilization of ATT on the paper-based chip's working electrode, a layer of graphene oxide was coated. First, 1 g of graphene oxide powder was dispersed in 99 mL of deionized (DI) water by ultrasonic vibration for 2 h until the 1% wt graphene oxide solution became

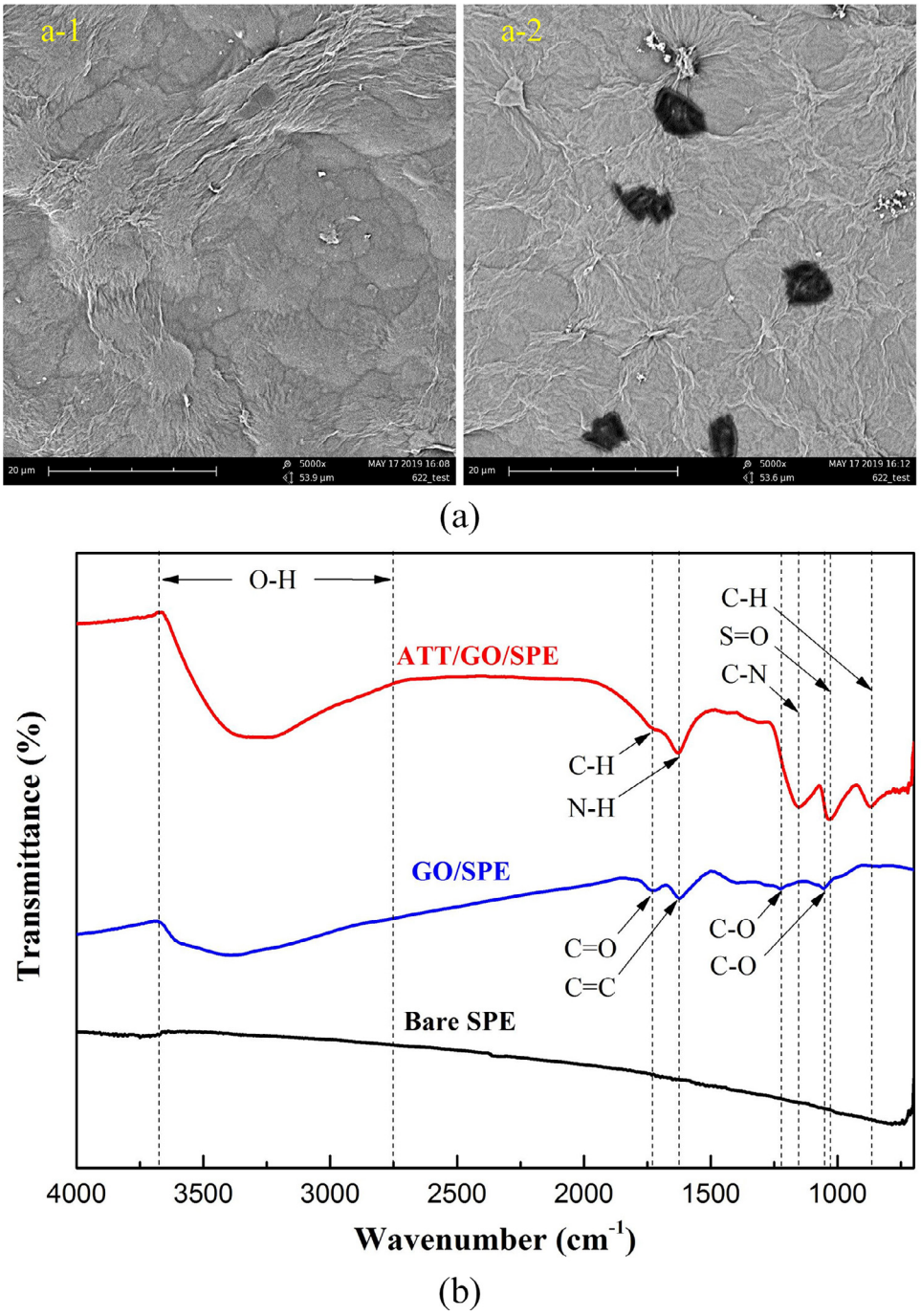

Fig. 2. (a) The SEM image of ATT (the black substances) on the surface of GO/SPE. (b) The FTIR spectrum of ATT/GO/SPE.

colloid. Then, 4 μL of colloid was drop cast on the electrode, and the paper-based chip was heated in a 37°C hot circulator oven for 1 h. This chip is labeled as GO/SPE.

Next, 0.133 g of ATT powder was mixed with 0.1 M H_2SO_4 (i.e., 10 mL of sulfuric acid with 90 mL of DI water) to form a 10 mM ATT solution. Moreover, 200 μL of this solution was drop cast on GO/SPE's electrode and electropolymerized by 30 successive potential cycles between −0.4 and +1.8 V at a scan rate of 50 mV/s. Finally, the paper-based chip was dried in a 37°C hot circulator oven for 3 h. This chip is labeled as ATT/GO/SPE. The photo in **Fig. 1a** shows the result of the ATT electropolymerization on the working electrode of the paper-based chip (i.e., ATT/GO/SPE).

CV experiment to detect uric acid

To prepare a certain concentration of uric acid for the experiment, the $C_5H_4N_4O_3$ powder was added in 0.1 M PBS and stirred using an ultrasonicator until it was thoroughly dissolved. Then, 200 μL of analyte solution was drop cast on the electrode of ATT/GO/SPE for CV measurement.

The CV curve and the oxidation wave were observed with 5 successive potential cycles between −0.2 and +1.7 V at a scan rate of 50 mV/s. However, the data of the first cycle were not taken into account. The CV curve was drawn using the average of the subsequent cycles.

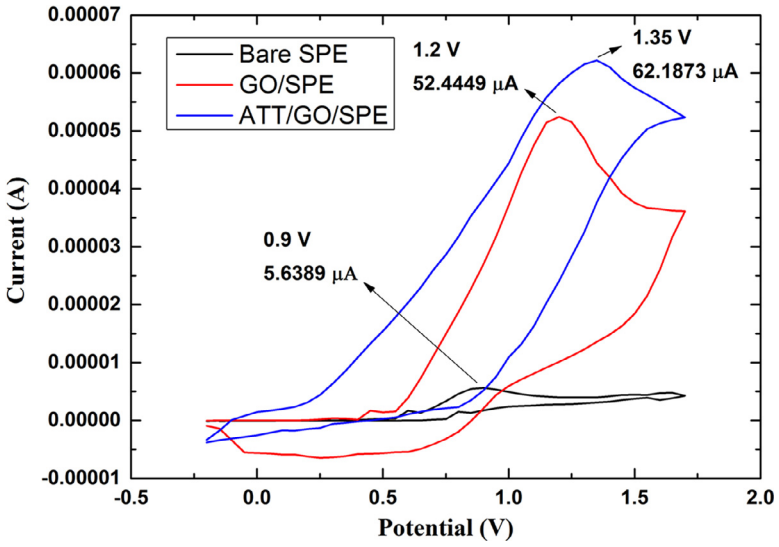

Fig. 3. The comparison of oxidation peak currents of uric acid performed at bare SPE, GO/SPE and ATT/GO/SPE, respectively.

To evaluate the performance of this proposed ATT/GO/SPE biosensor in detecting uric acid, many assays were carried out in this study, including measurement of different uric acid levels, anti-interference study, and effect of scan rate.

Results and discussion

ATT immobilization

The immobilization of ATT on the paper-based chip is a prerequisite for ATT/GO/SPE biosensor. Several tests were then conducted to check the characterization of ATT electropolymerization.

Raman spectrum of GO

The structure of GO is complicated with different kinds of oxygen species and bonds, such as epoxy, hydroxyl, and carbonyl groups, to carbon in the graphene layer. In addition, different synthesis methods lead to different types of graphene oxide. Therefore, Raman analysis was performed to investigate the defective states of the synthesized GO in this study.

The Raman spectrum of GO consists of two distinct peaks (i.e., D and G bands) representing two typical Raman active vibration modes in graphitic structures. The D band at 1350 cm^{-1} is related to the defects in the sp^2-bonded carbon network of GO, coming through the preparation process of GO. At around 1580 cm^{-1}, the G band is usually associated with the E_{2g} phonons allowed within the sp [2] network, describing the symmetry in crystals. As shown in **Fig. 1b**, the intensity ratio of the D peak to G peak (I_D/I_G), which predicts the degree of impurities within the GO basal plane, is equal to 0.9995. It explains that this as-prepared GO powder has pure crystals, and there are fewer defects intercalated in the sp [2] plane. Excessive destruction of the GO crystal structure due to the defects in the sp^2-bonded carbon network will be detrimental to the adsorption of ATT. Moreover, insufficient epoxide groups can also lead to infirm adsorption of ATT to the GO surface. The Raman analysis disclosed that the GO powder synthesized in this study had the potential to immobilize ATT.

Scanning electron microscope (SEM)

The immobilization of ATT on the surface of GO/SPE was directly examined using Phenom G2 pro desktop SEM. **Figures 2a-1** and **2a-2** show the topographic details on the surface of GO before and after the step of ATT electropolymerization, respectively. These SEM images are of 5000-magnification. White granular particles can be found on the graphene oxide before the electropolymerization step. Additionally, the white granular particles can still be observed after the step of ATT electropolymerization, while many larger black substances appear in the image. Thus, the inference drawn from the SEM results is that the white granular particles are obviously the particle contamination and the black substances on the surface of GO/SPE are ATT.

Fourier-transform infrared spectroscopy (FTIR)

To further confirm the success of ATT electropolymerization onto the surface of GO/SPE, the FTIR spectroscopy analysis was carried out to study the interaction between ATT and GO using the JASCO FT/IR-4700 FT-IR spectrometer and IRT-5200 FT-IR microscope. The IR spectra of bare SPE, GO/SPE, and ATT/GO/SPE were recorded for comparison.

When infrared radiation interacts with an organic compound, certain frequencies of energy, basically in the region of 4000 cm^{-1} to 1300 cm^{-1}, are absorbed due to the functional groups present in the substance. Hence, peaks that occurred in this spectroscopic region are characteristic of specific kinds of bonds. As shown in **Fig. 2b**, there is no characteristic band for bare SPE. However, the FTIR spectrum of GO/SPE shows a strong absorption band within the region 3665–2750 cm^{-1} due to the stretching of the hydroxyl (O–H) group. In addition, the peak at 1730 cm^{-1} is ascribed to the C=O carbonyl stretching, the skeletal stretching of the C=C alkene group at 1622 cm^{-1}, and the C–O epoxide group stretching at 1225 and 1055 cm^{-1}. All characteristic peaks of GO agree with those in the previous reports. [32,33]

From the FTIR spectrum of ATT/GO/SPE, it can be found that the intensities of many peaks are enhanced. The chemical formula of ATT is $=C_2H_3N_3S_2$. From the basic FTIR information for the organic functional groups, the absorption band of the stretching N–H group is in the region of 3400–3300 cm^{-1}. Hence, the high intense absorption band at 3665–2750 cm^{-1} in the FTIR spectrum of ATT/GO/SPE can be attributed to the stretching of O–H group of GO and the stretching of N–H group of ATT. That is, more infrared radiation was absorbed by the N–H group of ATT, except the O–H group of GO. Due to ATT electropolymerization onto the surface of GO/SPE, the peaks at 1730 and 1625 cm^{-1} are assigned to the bending of C–H and N–H groups, respectively. Moreover, the bands detected at 1153, 1033, and 870 cm^{-1} are characteristic peaks of C–N, S=O, and C–H, respectively. All these peaks present in the FTIR spectrum of ATT/GO/SPE explain that ATT was immobilized onto the surface of GO/SPE by electropolymerization.

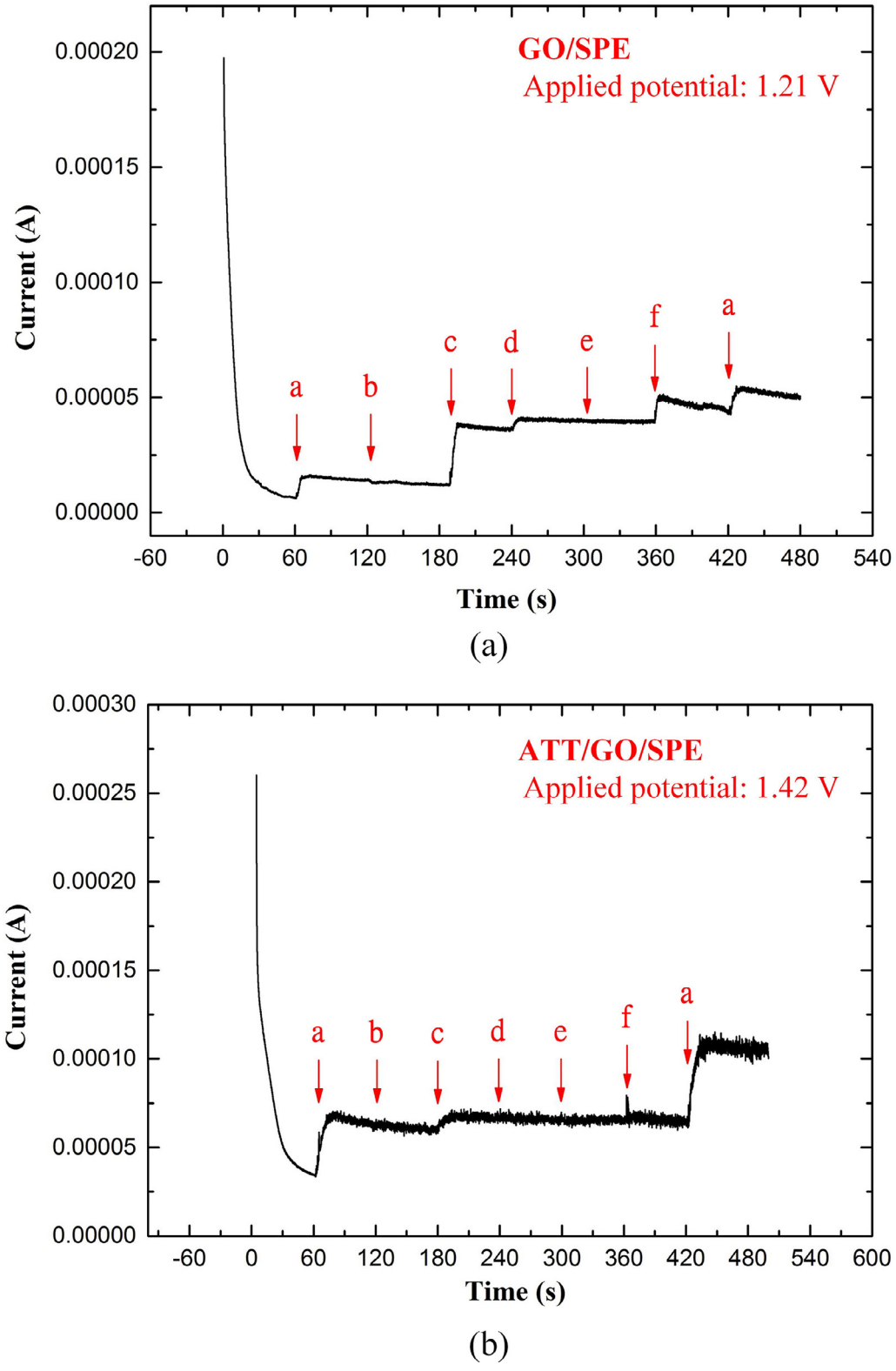

Fig. 4. Anti-interference study: (a) The responses of GO/SPE, many chemicals are observed to be interference factors. (b) The responses of ATT/GO/SPE, nitrite is an interference factor to uric acid.

Comparison of different electrodes

These three different kinds of modified working electrodes in detecting 3 mM uric acid were then compared. The electrochemical behavior of uric acid on the surface of the electrode was evaluated using CV measurements. The CV tests were carried out in the potential range of −0.2 ~ +1.7 V, in cyclical phases, at a scanning rate of 50 mV/s. The cyclic voltammograms were recorded.

As shown in Fig. 3, no characteristic peak which can be attributed to the oxidation of uric acid appeared at bare SPE. However, at the

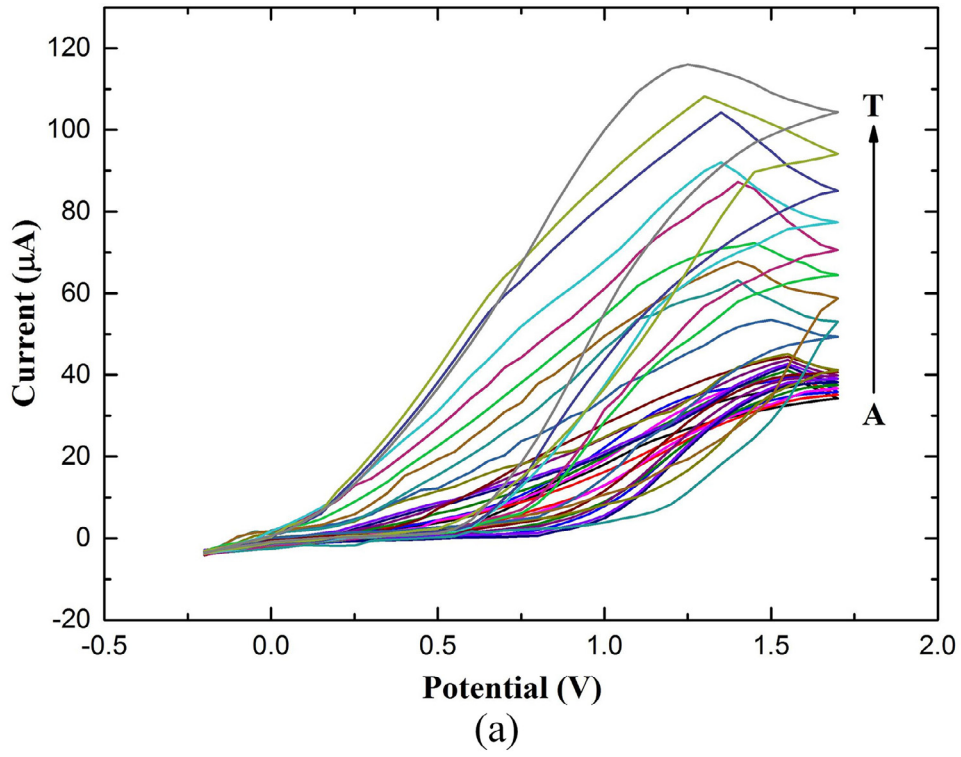

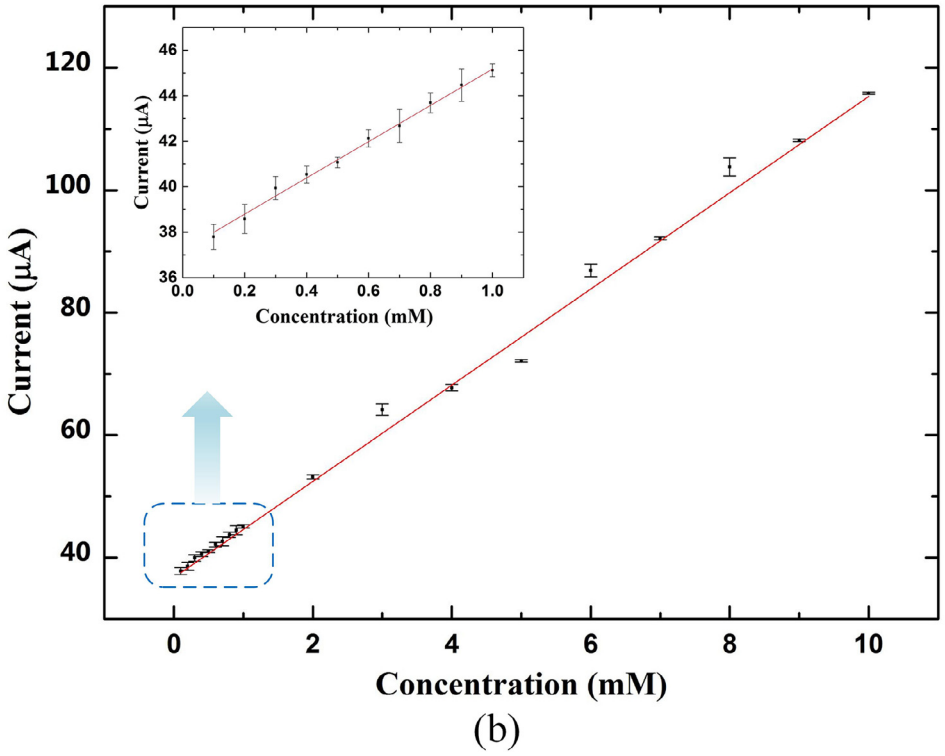

Fig. 5. Measurements of uric acid levels: (a) The cyclic voltammograms of different concentrations of uric acid. (b) The peak currents of different concentrations of uric acid.

GO/SPE, an irreversible oxidation peak appeared at 1.2 V with a peak current of 52.445 μA. The oxidation potential of uric acid at the surface of ATT/GO/SPE shifted to 1.35 V, with the peak current enhanced to 62.187 μA. Both the oxidation peak currents of uric acid at GO/SPE and ATT/GO/SPE are significantly enhanced in contrast to bare SPE. In addition, the peak current of uric acid at ATT/GO/SPE is larger than that at GO/SPE. Nevertheless, the oxidation peak potentials were shifted toward more positive potentials for both GO/SPE and ATT/GO/SPE due to the coating of GO and ATT on the bare SPE.

Anti-interference study

From the above experimental results, both GO/SPE and ATT/GO/SPE seem suitable for detecting uric acid since their oxidation

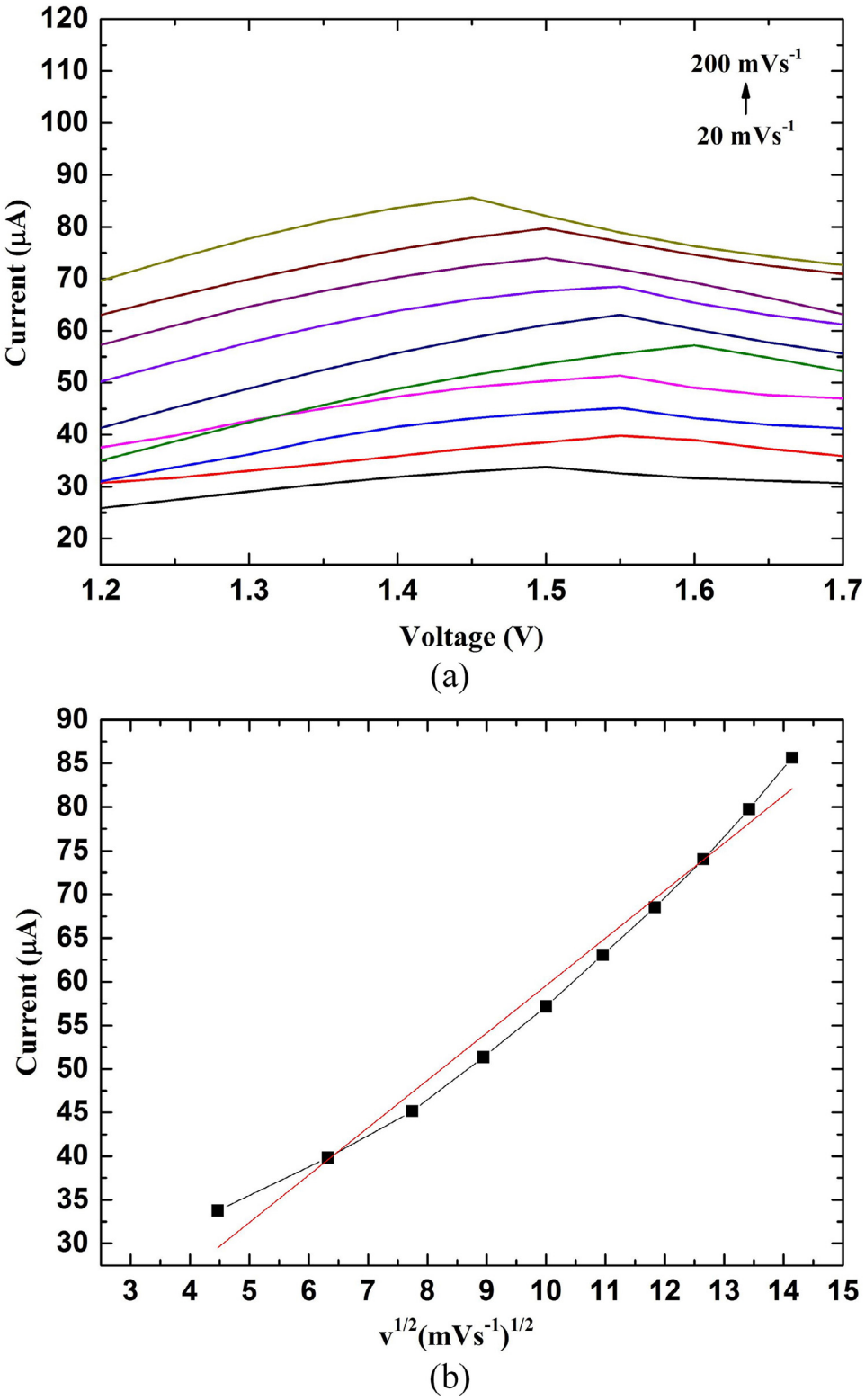

Fig. 6. Effect of scan rate: (a) The oxidation peak currents at different scan rates. (b) The relationship between the oxidation peak current and the square root of the scan rate.

peaks are significantly enhanced. Therefore, further investigation is required.

The anti-interference is an essential assay because some chemicals, such as ascorbic acid (AA), nitrite, glucose, dopamine (DA), and red blood cell (RBC), may coexist with the uric acid in human blood and body fluids. Good selectivity and high sensitivity in detecting uric acid levels without suffering from the influences generated from these chemicals are the most important requirements in practical clinical applications. In this study, chronoamperometric measurements were performed using GO/SPE and ATT/GO/SPE by adding the aforementioned chemicals to 0.1 M PBS (pH: 7.0, 200 mL) solution at their oxidation potentials of uric acid, respectively. The sequence of successive addition of chemicals (every 60 s) was: (a) 0.2 mM UA, (b) 0.1 mM AA, (c) 1 mM nitrite, (d) 1 mM glucose, (e) 0.1 mM DA, and (f) 3% 1 mL RBCs. The concentra-

tion set for experiments was chosen based on the actual concentration of each chemical in the human blood.

As shown in Fig. 4**a**, the amperometric *i–t* curve indicates the responses of GO/SPE upon successively adding the aforementioned chemicals. Initially, a significant rise of current due to the addition of the uric acid indicates that the oxidization response occurred on the electrode. However, many chemicals are interference factors, including (c) nitrite, (d) glucose, and (f) RBCs. A rise of current popped up whenever an interference factor was added, which means that GO/SPE does not have good selectivity to detect uric acid because GO does not have specific binding to it.

The amperometric *i–t* curve in Fig. 4**b** shows the responses of ATT/GO/SPE upon successive addition of these chemicals. The addition of (c) nitrite caused a slight rise of current, while a current pulse was observed after adding (f) RBCs. However, no evident signal changes were found for the other chemicals. The results reveal that nitrite has interference with uric acid. This proposed ATT/GO/SPE biosensor utilizes ATT to capture uric acid for measurement. The functional group of ATT can also bind with nitrite ions, resulting in interference. Although nitrite is an interference factor to uric acid, it can be discriminated from uric acid in the CV measurements. The oxidation potential of nitrite is 0.8 V, while the uric acid is oxidized at 1.4 V. In addition, although RBCs are another interference factor to uric acid, they did not produce a redox reaction at ATT/GO/SPE in the applied potential range during the CV measurements. Therefore, only a current pulse was observed. Based on the above experimental results, it can be concluded that ATT electropolymerization to GO/SPE is a necessary step for UA detection to reduce the interferences from other components in human blood and body fluids. ATT/GO/SPE biosensor exhibits a better selectivity and sensing performance towards the detection of uric acid than the GO/SPE biosensor.

Measurement of different uric acid levels

To investigate the applicability of ATT/GO/SPE in determining uric acid levels, different uric acid concentrations were employed and measured with CV. Since the physiological concentration of uric acid present in the blood is about 3–7 mg/dL (i.e., 0.15–0.45 mM), a series of concentrations beginning from 0.1 to 10 mM were designed for CV tests. For each concentration, three ATT/GO/SPE biosensors were prepared for the purpose of repetitious experiments.

Fig. 5**a** shows the cyclic voltammograms of uric acid in different concentrations, and the oxidation peak current increased noticeably as the concentration of uric acid increased. However, the oxidation potential slightly decreased as the concentration of uric acid increased. Such implies that the oxidization reaction is prone to a higher concentration of uric acid on the electrode. As shown in Fig. 5**b**, the peak current exhibits a linear relationship with the concentration of uric acid. Its linear regression equation is defined as

$$I_p = 7.857C_{UA} + 36.729,$$

where I_p denotes the peak current while C_{UA} is the concentration of uric acid. The coefficient of determination R^2 reaches 0.997. The sensitivity number of this biosensor is 7.857 μA/mM. The inset of Fig. 5**b** illustrates the linear relationship in the concentration range of 0.1–1.0 mM. The experimental result reveals that this proposed ATT/GO/SPE biosensor is applicable for detecting the uric acid level in the range of physiological concentration, as well as the range of higher concentration.

Effect of scan rate

To evaluate the effect of scan rate on the oxidation of uric acid at ATT/GO/SPE, linear sweep voltammetry (LSV) was performed using a 1 mM uric acid solution. The potential between the working electrode and the reference electrode was swept linearly in time from −0.2 to +1.7 V. Meanwhile, the scan rate was changed from 20 to 200 mV/s with an interval of 20 mV/s. As shown in Fig. 6**a**, the oxidation peak current of uric acid increased with the scan rates. Good linearity between the oxidation peak current and the square root of the scan rate was obtained, as shown in Fig. 6**b**. This experimental result is in accordance with the Randles-Sevcik equation, indicating that the uric acid reaction at ATT/GO/SPE is a diffusion-controlled process in the investigated range.

Conclusion

Gout and hyperuricemia, prevalent globally in recent years, are usually associated with a variety of chronic diseases. For these patients, their uric acid levels must be monitored or maintained using medicines. In this study, a paper-based biosensor modified with GO and ATT was developed to determine uric acid levels. While this proposed biosensor has many advantages, the fabrication process is also simple. It requires only a small quantity of analyte solution for an experiment. Moreover, this biosensor has high sensitivity in detecting the uric acid level in the range of physiological concentration, as well as the range of higher concentration. It also has good selectivity without suffering from the influences generated from the other chemicals in human blood and body fluids. Therefore, it could be a perfect candidate for detecting uric acid to monitor physiological disorders.

Supporting Information

Synthesis of graphene oxide

The graphene oxide was synthesized from graphite powder using a modified Hammer's method. The first synthesis step was to dissolve 1 g of sodium nitrate in 80 mL sulfuric acid (98%) in a flask placed in an ice bath with constant stirring for 1 h, followed by adding 2 g of graphite powder with stirring for an additional 1 h. Afterwards, 8 g of potassium permanganate was slowly added to the solution mixture with stirring for 3 h until the color of the solution became dark green. The solution was then transferred to a 40°C water bath with stirring for 6 h. Subsequently, 100 mL of DI water was slowly added to the solution using a syringe pump; meantime, the temperature of the solution was maintained under 100°C. Next, the solution was heated in a 98°C hot circulator oven for 20 min. Finally, the addition of 30 mL of hydrogen peroxide (30%) to the solution was conducted to react with the redundant potassium permanganate. When the color of the solution became bright yellow, the basic synthesis step was accomplished. The as-prepared product was rinsed with hydrochloric acid (5%) and DI water several times, followed by the centrifugal process to discard the supernatant. After centrifugation, the precipitate was packed in a dialysis membrane and then placed in a DI water bath for 7 days. The final product was dried at low temperature to form a powder.

Declaration of Conflicting Interests

The authors declared no potential conflicts of interest with respect to the research, authorship, and/or publication of this article.

Acknowledgement

This work was supported by the Ministry of Science and Technology (MOST) of Taiwan, R.O.C. [grant number MOST 109-2221-E-033-014]

References

[1] Grabowska I, Chudy M, Dybko A, et al. Uric Acid Determination in a Miniaturized Flow System with Dual Optical Detection. Sens Actuators B-Chem 2008;130:508–13.
[2] Herrasti Z, Martínez F, Baldrich E. Detection of Uric Acid at Reversibly Nanostructured Thin-Film Microelectrodes. Sens Actuators B-Chem 2016;234:667–73.
[3] Pucetaite M, Velicka M, Pilipavicius J, et al. Uric Acid Detection by Means of SERS Spectroscopy on Dried Ag Colloidal Drops. J Raman Spectrosc 2016;47:681–6.

[4] Yu K-H, Chen D-Y, Chen J-H, et al. Management of Gout and Hyperuricemia: Multidisciplinary Consensus in Taiwan. Int J Rheum Dis 2018;21:772–87.
[5] Norazmi N, Abdul Rasad ZR, Mohamad M, et al. Uric Acid Detection Using Uv-Vis Spectrometer. IOP Conf Ser: Mater Sci Eng 2017;257:012031 6 pp.
[6] Chen Z, Zu Y. Selective Detection of Uric Acid in the Presence of Ascorbic Acid Based on Electrochemiluminescence Quenching. J Electroanal Chem 2008;612:151–5.
[7] Tao Y, Zhang X, Wang J, et al. Simultaneous Determination of Cysteine, Ascorbic Acid and Uric Acid by Capillary Electrophoresis with Electrochemiluminescence. J Electroanal Chem 2012;674:65–70.
[8] Ballesta-Claver J, Rodríguez-Gómez R, Capitán-Vallvey LF. Disposable Biosensor Based on Cathodic Electrochemiluminescence of Tris(2,2-bipyridine)ruthenium(II) for Uric Acid Determination. Anal Chim Acta 2013;770:153–60.
[9] Goodall BL, Robinson AM, Brosseau CL. Electrochemical-Surface Enhanced Raman Spectroscopy (E-SERS) of Uric Acid: A Potential Rapid Diagnostic Method for Early Preeclampsia Detection. Phys Chem Chem Phys 2013;15:1382–8.
[10] Popa E, Kubota Y, Tryk DA, et al. Selective Voltammetric and Amperometric Detection of Uric Acid with Oxidized Diamond Film Electrodes. Anal Chem 2000;72:1724–7.
[11] Sheng Z-H, Zheng X-Q, Xu J-Y, et al. Electrochemical Sensor Based on Nitrogen Doped Graphene: Simultaneous Determination of Ascorbic Acid. Dopamine and Uric Acid. Biosens Bioelectron 2012;34:125–31.
[12] Ali M, Shah I, Kim SW, et al. Quantitative Detection of Uric Acid Through ZnO Quantum Dots Based Highly Sensitive Electrochemical Biosensor. Sens Actuator A-Phys 2018;283:282–90.
[13] Zhou Q, Lin Y, Shu J, et al. Reduced Graphene Oxide-Functionalized FeOOH for Signal-On Photoelectrochemical Sensing of Prostate-Specific Antigen with Bioresponsive Controlled Release System. Biosens Bioelectron 2017;98:15–21.
[14] Zhang K, Lv S, Zhou Q, et al. CoOOH Nanosheets-Coated g-C_3N_4/$CuInS_2$ Nanohybrids for Photoelectrochemical Biosensor of Carcinoembryonic Antigen Coupling Hybridization Chain Reaction with Etching Reaction. Sens Actuators B-Chem 2020;307:127631.
[15] Yang G, Li L, Jiang J, et al. Direct Electrodeposition of Gold Nanotube Arrays of Rough and Porous Wall by Cyclic Voltammetry and Its Applications of Simultaneous Determination of Ascorbic Acid and Uric Acid. Mater Sci Eng C-Mater Biol Appl 2012;32:1323–30.
[16] Zhao D, Yu G, Tian K, et al. A Highly Sensitive and Stable Electrochemical Sensor for Simultaneous Detection Towards Ascorbic Acid, Dopamine, and Uric Acid Based on the Hierarchical Nanoporous PtTi Alloy. Biosens Bioelectron 2016;82:119–26.
[17] Savk A, Özdil B, Demirkan B, et al. Multiwalled Carbon Nanotube-Based Nanosensor for Ultrasensitive Detection of Uric Acid, Dopamine, and Ascorbic Acid. Mater Sci Eng C-Mater Biol Appl 2019;99:248–54.
[18] Liu X, Zhang L, Wei S, et al. Overoxidized Polyimidazole/Graphene Oxide Copolymer Modified Electrode for the Simultaneous Determination of Ascorbic Acid, Dopamine, Uric Acid, Guanine and Adenine. Biosens Bioelectron 2014;57:232–8.
[19] Zhou X, He Z, Lian Q, et al. Simultaneous Determination of Dihydroxybenzene Isomers Based on Graphene-Graphene Oxide Nanocomposite Modified Glassy Carbon Electrode. Sens Actuators B-Chem 2014;193:198–204.
[20] Ahour F, Ahsani MK. An Electrochemical Label-Free and Sensitive Thrombin Aptasensor Based on Graphene Oxide Modified Pencil Graphite Electrode. Biosens Bioelectron 2016;86:764–9.
[21] Gevaerda A, Blaskieviczb SF, Zarbinc AJG, et al. Nonenzymatic Electrochemical Sensor Based on Imidazole-Functionalized Graphene Oxide for Progesterone Detection. Biosens Bioelectron 2018;112:108–13.
[22] Shu J, Qiu Z, Tang D. Self-Referenced Smartphone Imaging for Visual Screening of H2S Using CuxO-Polypyrrole Conductive Aerogel Doped with Graphene Oxide Framework. Anal. Chem. 2018;90:9691–4.
[23] Zeng R, Luo Z, Zhang L, et al. Platinum Nanozyme-Catalyzed Gas Generation for Pressure-Based Bioassay Using Polyaniline Nanowires-Functionalized Graphene Oxide Framework. Anal. Chem. 2018;90:12299–306.
[24] Zhou Q, Lin Y, Zhang K, et al. Reduced Graphene Oxide/$BiFeO_3$ Nanohybrids-Based Signal-On Photoelectrochemical Sensing System for Prostate-Specific Antigen Detection Coupling with Magnetic Microfluidic Device. Biosens Bioelectron 2018;101:146–52.
[25] Fatma S, Prasad BB, Jaiswal S, et al. Electrochemical Simultaneous Analysis of Dopamine and Epinephrine Using Double Imprinted One MoNomer Acryloylated Graphene Oxide-Carbon Black Composite Polymer. Biosens Bioelectron 2019;135:36–44.
[26] Zhu G, Zhang X, Chen J. Sensitive Electrochemical Sensor of Anthracene-9-Carbonxylic Acid Using an Electropolymerized Film Modified Glassy Carbon Electrode. Anal Methods 2013;5:1881–5.
[27] Rajalakshmi K, Abraham John S. Highly Sensitive Determination of Nitrite Using FMWCNTs-Conducting Polymer Composite Modified Electrode. Sens Actuators B-Chem 2015;215:119–24.
[28] Yun M, Choe JE, You JM, et al. High Catalytic Activity of Electrochemically Reduced Graphene Composite Toward Electrochemical Sensing of Orange II. Food Chem 2015;169:114–19.
[29] Xia Y, Si J, Li Z. Fabrication Techniques for Microfluidic Paper-Based Analytical Devices and Their Applications for Biological Testing: A Review. Biosens Bioelectron 2016;77:774–89.
[30] Panraksa Y, Siangproh W, Khampieng T, et al. Paper-Based Amperometric Sensor for Determination of Acetylcholinesterase Using Screen-Printed Graphene Electrode. Talanta 2018;178:1017–23.
[31] Sánchez-Calvo A, Núñez-Bajo E, Fernández-Abedul MT, et al. Optimization and Characterization of Nanostructured Paper-Based Electrodes. Electrochim Acta 2018;265:717–25.
[32] Sabagh S, Aref Azar A, Bahramian AR. High Temperature Ablation and Thermo-Physical Properties Improvement of Carbon Fiber Reinforced Composite Using Graphene Oxide Nanopowder. Compos Pt A-Appl Sci Manuf 2017;101:326–33.
[33] Amrollahi S, Ramezanzadeh B, Yari H, et al. Synthesis of Polyaniline-Modified Graphene Oxide for Obtaining a High Performance Epoxy Nanocomposite Film with Excellent UV Blocking/Anti-Oxidant/ Anti-Corrosion Capabilities. Compos Pt B-Eng 2019;173:106804 14 pp..